Chapter 3

Polysaccharide Fucoidan Fabricated Bosutinib Nanocrystals for Pulmonary Drug Delivery: Solid State Characterization and *In-vitro* Assessment

Chapter 3. Polysaccharide Fucoidan Fabricated Bosutinib Nanocrystals for Pulmonary Drug Delivery: Solid State Characterization and In-vitro Assessment

3.1. Rationale

Lung cancer is top most common cancer and the leading cause of cancer-related death worldwide (mainly in the United States). According to the American Cancer Society, the chances of survival for five years is only 16-25 % (distant stage cancer only 6 %). Lung cancer has been reported for the highest mortality rate (31.8 %) compared to other cancers (USCS Data Visualizations). Among lung cancers, 80-85 % of lung cancers are non-small cell lung cancer (NSCLC). NSCLC has been shown over the past several years to contain mutations in specific oncogenes, responsible for high mortality rates. Tyrosine kinase inhibitors (TKIs) have recently gained widespread popularity in early and late-stage lung cancer treatment. TKIs can be combined with conventional treatment to provide better therapeutic (Kumar and Rajnikanth, 2020). Bosutinib is such TKI that can potentially inhibit mutated oncogenes responsible for advanced-stage cancer (Isakoff et al., 2014). Bosutinib can inhibit ACK1, which attenuates migration and invasion in the context of KRAS mutant NSCLC to fulfil a therapeutic niche through combinatorial treatment approaches (Tan et al., 2014). Bosutinib is also reported to inhibit Src overexpressed in NSCLC for improved patient survival (Karim et al., 2022). Although bosutinib has been reported for cancer therapy, the clinical outcomes are limited due to poor aqueous solubility and permeability. Bosutinib belongs to BCS Class IV drug, exhibiting poor drug bioavailability of only 34 % (Famta et al., 2023; Hsyu et al., 2018; Shah et al., 2024). This necessitated the development of a dosage form that can effectively improve the drug delivery.

Drug nanocrystals have recently gained widespread popularity owing to their high payload, solubility, permeability, and stability (Kumar et al., 2020b, 2019d, 2019b). In

addition, pulmonary delivery of drug nanocrystals ensures localized drug delivery to the lungs for better therapeutic effects. Pulmonary delivery has gained popularity for local and systemic action. Drug nanocrystals can offer high drug dissolution, excellent aerosolization performance, enhanced mucus penetration, good lung tissue distribution, and minimal drug clearance on pulmonary administration (He et al., 2020b; Kumar et al., 2020a). Drug nanocrystals can escape the clearance mechanism by their size-dependent dissolution and permeation (Kaur et al., 2022; Kumar et al., 2020a). Nanocrystals has advantages over nebulizers due to higher physical stability, portability, and ease of use (He et al., 2020b; Kumar et al., 2020a). Therefore, the formulation of bosutinib as a drug nanocrystal benefits pulmonary administration as dry powder.

3.2. Objective

The present work proposed the formulation of bosutinib nanocrystals (FBNC) using marine biopolymer fucoidan as stabilizer. The formulated nanocrystals were evaluated for their particle characteristics (size, polydispersity index, zeta potential and drug content). Microscopic investigations (SEM, AFM, and TEM) and solid-state characterizations (including FTIR, DSC, XRD, XPS, solid-state NMR and BE). The in-vitro drug release in simulated lung fluid (SLF), in-vitro simulated mucus diffusion, and in-vitro aerosolization studies were also conducted for in-vitro assessment of performance of drug nanocrystals towards pulmonary drug delivery.

3.3. Materials

Bosutinib was received as a gift sample from MSN Laboratories Private Limited Unit II, Telangana-502300, India. Fucoidan (*Undaria pinnatifida*) of medicine grade was gifted by Nutra Green Biotechnology, Co., Ltd. Shanghai-200129, China. Acetonitrile

and water of HPLC grade were procured from Finar chemicals, India. All other chemicals used were of Analytical reagent grade.

3.4. Methods

3.4.1. Preparation of Bosutinib Nanocrystals

Bosutinib nanocrystals (FBNC) were prepared by a slightly modified nanoprecipitation method (Kumar et al., 2019d). Fucoidan (1 % w/v) was used as a dispersion stabilizer maintained at a lower temperature (about 2-8 °C) in ice-cold water under continuous stirring at 2000 rpm. To prepare nanocrystals, 1 ml of bosutinib ethanolic solution (10 mg/ml) was added to 10 ml of aqueous fucoidan solution drop-by-drop using a 2 ml syringe fitted with 24 G Needle. Rapid addition of organic phase to aqueous phase resulted in immediate precipitation from antisolvent. Continuous stirring aided in the uniform distribution of drug solution while lower temperature favouring the immediate crystallization, resulting in a uniform-size distributed particle. The resultant dispersion was probe sonicated (UP50H, Ultrasonic Processor, Hielscher Ultrasound Technology, Germany) for 10 min at pulse rate 07/03 and amplitude 50 % while maintaining the dispersion in ice-cold water to bring particles in the desired nano-range. The formulations were kept on stirring at 200 rpm overnight at room temperature. The resultant nanocrystals were collected by centrifugation for 15 min at -4 °C and 15000 rpm using a high-speed cooling centrifuge. The collected nanocrystals were lyophilized to obtain the dry powder of nanocrystals, kept overnight in desiccator and then stored in refrigerator (2-8 °C) until further use.

3.4.2. Evaluation of Nanocrystals

Particle size and zeta potential of FBNC were determined by dynamic light scattering (DLS) using Zetasizer (Nano ZS, Malvern Instruments, Malvern, UK). The formulation

was diluted ten times with deionized water before measurements (Soisuwan et al., 2019).

The drug content (DC) of nanocrystals was measured by HPLC. A reverse-phase HPLC column (C18) was used. Briefly, 100 mg of lyophilized powder was added to 5 ml of methanol and vortexed for 10 minutes for stabilizer membrane disruption. The solution was then centrifuged at 15000 rpm for 10 min, and the supernatant was collected and filtered through a 0.20 μm syringe filter. The flow rate of the mobile phase of ACN-Buffer pH 5.8 (48:52 v/v) was set at 1.0 ml/min. The column effluent was detected with a UV/VIS detector at 267 nm. The calibration curve was linear in the 10–10,000 ng/ml range, with a correlation coefficient of $R^2 = 0.999$. The DC was defined as the ratio of the drug in nanocrystals to the weight of nanocrystals used. Robustness to dilution was also checked to determine the effect of dilution on nanocrystal size. For this, 1 mg/ml nanocrystals were diluted 10, 20, and 50-fold and bath sonicated for 30 sec to disperse the particle homogeneously.

Then, the particle size was measured using Zetasizer at various time points (Deng et al., 2010). The storage stability of lyophilized samples of nanocrystals was also analysed. For this, samples were resuspended in PBS and measured for particle size, PDI, zeta potential, and drug content at predetermined time intervals (day 1, 7, 15, 30, 90, and 180) (Ruttala and Ko, 2015). The residual moisture content in lyophilized nanocrystals pre- and post-storage was also determined through Karl Fischer titration method (USP 921 General Chapter on Water Determination) (Jameel et al., 2021). For this, sample (100 mg of nanocrystals) was transferred to Karl Fischer Titrator (KAFI+, Labindia) and analysis was performed as per the instructions provided by manufacture (Merckx et al., 2020).

The surface characteristics like shape, morphology, and roughness were determined using an EVO scanning electron microscope (SEM) (MA15/18, CARL ZEISS Microscopy Ltd.) and scanning probe microscope (SPM) (NTEGRA Prima, NT-MDT Service, and Logistics Ltd). For sample preparation, the formulation was diluted 20 folds with distilled water, dropped onto the glass slides, and then vacuum dried overnight at 25 °C. The dried samples were used for SPM analysis, and measurements were done using Nova Powerscript 3.4.0 rev 16681 as SPM image analysis software. For SEM, dried samples were coated with gold for 120 sec using a rotary pumped sputter coater and characterized. High-Resolution Transmission Electron Microscope (HR-TEM, Tecnai G2 20 TWIN, FEI Corporation of USA (S.E.A.) PTE, LTD) was used to determine nanocrystal size. The TEM grid was prepared by dropping a 20-fold diluted nanoformulation on a 200-mesh copper grid (AGS160, Agar Scientific Ltd.) and dried at room temperature overnight.

3.4.3. Solid State Characterization

Solid-state characterization of Coarse drug (BTB), fucoidan (FP) and bosutinib nanocrystals (FBNC) was done using FTIR, powder X-ray diffraction (XRD), differential scanning calorimetry (DSC), X-ray photoelectron spectroscopy (XPS), solid-state NMR, and Brunner-Emmett-Teller (BET). The FTIR study was conducted using SHIMADZU 8400S, Tokyo, Japan. For this, samples were triturated with KBr in 1:5 and pressed into pellets using a hydraulic press. The FTIR spectrum was recorded between 4000 cm^{-1} to 600 cm^{-1} at a resolution of 4 cm^{-1} and a scan rate of 64 accumulation per min. The change in the physical state of coarse drugs on processing to nanocrystals was studied using Rigaku Miniflex 600 powder x-ray diffractometer equipped with a D/teX Ultra detector. The diffraction pattern was recorded at a scan rate of 5º min^{-1} over the 2θ range of 5º to 50º at a rate of 5º of 2θ per min and step size

of 0.02º. The DSC analysis of samples was performed using Shimadzu DSC-60 Plus between the temperature range of -25 to 300 ℃ at a heating rate of 20 ℃/min and nitrogen purging at 40mL/min. XPS analysis was used to assess the surface chemistry of formulations using K-Alpha (Thermo Fisher Scientific) with Mg Kα radiation (hν = 1253.6 eV) in the range of 100-700 eV binding energy. Solid state NMR was done using Advance Neo 600 MHz NMR Spectrometer, Bruker India Scientific. The NMR data was collected for coarse drug (BTB), stabilizer fucoidan (FP), and nanocrystals (FBNC) and were assigned by ^{13}C NMR. The chemical shifts were expressed in parts per million (ppm). Brunauer-Emmett-Teller (BET) was conducted to determine the effective surface area using the nitrogen adsorption method at 77.36 K using BELLSORP MAX II & BELCAT-II, MicrotracBEL Corp.

3.4.4. Saturation Solubility in Simulated Lung Fluid (SLF)

The equilibrium solubility of the coarse drug (BTB) and FBNC in simulated lung fluid (SLF) was measured using the Saturation shake-flask method (Kumar et al., 2019d). Simulated lung fluid comprising 0.02 % w/v DPPC, maintained at 35 ℃ (Williams RO et al., 2008). An excess sample was added to 10 ml of media shaken at 37 ± 0.5 ℃ in a water-bath shaker for 48 h to achieve equilibrium (Jiang et al., 2012). The equilibrated liquid was centrifuged for 15 min at 15000 rpm and filtered through a 0.2 µm syringe filter (AXIVA) to remove the surplus insoluble excipients. The filtrate was analyzed at 267 nm using HPLC.

3.4.5. Water Contact Angle

The water contact angle of nanocrystals was conducted to determine the wettability of nanocrystals compared to coarse drugs. The study was performed by static contact angle measurement instrument (KRUSS GmbH Germany, DSA 10). For this, lyophilized nanocrystals and the crude drug were punched into tablets (100 mg,

pressure 5 kg). For measurement, a drop of SLF (~4 µL) was dropped on the plane surface of the tablet through a microinjector, and the camera captured the image. The contact angle values were noted, and measurement was done in triplicate (Jiang et al., 2012).

3.4.6. In-Vitro Drug Dissolution in Simulated Lung Fluid

In-vitro drug dissolution of nanocrystals for pulmonary delivery was conducted in SLF (0.02 % w/v DPPC) (Williams et al., 2008). The modified dialysis bag diffusion technique was used for studying the in-vitro drug dissolution of FBNC. A 50 ml falcon tube with an open upper end and a lower end assembled with a dialysis bag (12 kD) was used for this. FBNC equivalent to 5 mg of bosutinib redispersed in 2 ml SLF was added to the falcon tube (donor compartment) immersed in 48 ml of SLF (acceptor compartment) in a beaker. The system was maintained at 37 ± 0.5 °C under continuous stirring at 100 rpm/min. At predetermined time intervals, aliquots of 2 ml were collected from the acceptor compartment and replaced with the same volume of fresh medium. Bosutinib has poor aqueous solubility in phosphate-buffered saline. Therefore, 0.1 % (w/v) Tween 80 was added in the dissolution medium to maintain the sink condition. The samples were filtered through a 0.20 µm syringe filter before analysis for drug content by HPLC.

3.4.7. In-Vitro Mucus Diffusion

The capability of FBNC to diffuse across lung mucus layer was assessed using a vertical Franz diffusion cell (He et al., 2020b; Khan et al., 2021). This experiment used 0.5 % HEC solution as simulated mucus due to its close resemblance to mucin in terms of chemical and microrheological properties. Briefly, a pair of polycarbonate filters (Merck Millipore, 2 µm) as diffusion membrane was fixed to the donar compartment of Franz cell, and the gap between the filters was filled with 20 µL of 0.5 % HEC solution.

The effective diffusion area of this setup was 1square cm. The acceptor compartment was filled with 7.5 mL phosphate buffer (pH 7.4) containing 0.2 % sodium dodecyl sulphate solution, and the experiment was started by adding 1 mL FBNC (equivalent to 1 mg BTB) into the donor compartments. The device was maintained at 37 °C with a circulating water bath. After 1 h and 6 h of diffusion, the sample was collected from the acceptor chamber. The sample was centrifuged at 15000 rpm for 10 min at -4 °C to collect the nanocrystals permeated across the diffusion membrane. The sediment was redispersed in distilled water and analyzed for possible intact nanocrystals using Zetasizer. The supernatant collected and redispersed sediment was used for determining the amount of drug diffused across the membrane using HPLC.

3.4.8. Powder Flow Study

The flowability of prepared nanocrystals (FBNC) was determined using angle of repose method in General Chapter <1174> Powder Flow in United States of Pharmacopeia (USP). For this, the lyophilized nanocrystals were converted to fine a dry powder of nanocrystals by rotating slowly clockwise in mortar pestle, without applying any pressure. Then, nanocrystals powder was poured from a height through a conical flask to form a static heap of powder. The height and radius of pile were noted and the angle of repose was calculated (Kumar et al., 2024a).

3.4.9 In-Vitro Aerosolization Performance

The aerosolization performance of nanocrystals was determined using a twin-stage impinger, apparatus A (TSI), *i.e.,* an artificial lung model (TSI, Apparatus, A; British Pharmacopeia, 2000) (Copley, UK). The Rotahaler®, a single-unit dose dry powder inhaler device, was chosen as a nanocrystal holder and delivery unit. HPMC capsule 3 was used for holding FBNC (equivalent to 20 mg BTB). The repairable fraction of FBNC was determined using TSI, comprised of an upper stage (upper airways) and

lower stage (lower airways) containing 7 ml and 30 ml of Methanol, respectively. Rotahaler with a filled capsule was attached to the rubber mouthpiece of TCI. The powder was aerosolized at 60 ± 5 L per min for 15 sec (5 sec×3) (Drumond et al., 2014). The fraction of nanocrystal powder in each stage was collected, dissolved in methanol, filtered, and analyzed by HPLC to determine the drug deposited at each location. The amount of drug deposited in the upper and lower stages was determined as emitted dose (ED). The amount of drug deposited in the lower stage was considered fine particle dose (FPD) and calculated as the percentage of ED deposited in stage 2. The respirable fraction (RF) was calculated as the ratio of FPD to ED and was expressed in percentage.

The aerosolization performance of BTB and FBNC were also determined using eight-stage Anderson cascade impactor (ACI, Westech Instruments, UK) recommended by the Ph. Eur. 6th edition for aerodynamic analysis. The powder (equivalent to 20 mg BTB) was filled in size 3 HPMC capsule (C) and loaded in the device (Rotahaler® Cipla, a commercially available single-dose capsule-based DPI). The inhaler device (D) was connected to the ACI using a mouthpiece adaptor (MP). The capsule was pierced into device prior to actuation in ACI. The test was carried out at a flow rate of 60 L/min and actuation time of 4 sec. Ten capsules were used in each run for each sample. Post aerosolization, the inhaler device, mouthpiece, induction port (I), pre-separator (PS) and all stages (Table 3.1) were washed using methanol and quantitatively determined by HPLC. Emitted dose (ED) was also determined from particles distributed at each stage of ACI and was the difference between the amount of powder filled into and the amount of powder remaining in the capsule within the DPI device. Fine particle fraction (FPF) was calculated as percentage of drug particles less than 5 μm, deposited at stages 2-7 of ACI. FPF is indicative of particles fraction that are suitable for effective

inhalation and assumed to deposit in the lungs to induce a pharmacological effect (Chvatal et al., 2017).

Table 3.1 Effective cut-off diameter of each stage of impactor.

Stage Number	**Stage 0**	**Stage 1**	**Stage 2**	**Stage 3**	**Stage 4**	**Stage 5**	**Stage 6**	**Stage 7**
Cut-off Diameter (µm)	8.6	6.5	4.4	3.2	1.9	1.2	0.6	0.3

3.5. Statistics

The results were presented as Mean ± SD. Statistical analysis like Two-tailed student t-test, one-way ANOVA and two-way ANOVA were performed for comparing groups. The significance was shown as "****" for $p < 0.0001$, "***" for $0.001 < p > 0.0001$, "**" for $0.01 < p > 0.001$, "*" for $0.05 < p > 0.01$ and "ns" for non-significant.

3.6. Results and Discussion

3.6.1. Preliminary Screening

Fucoidan, a hydrophilic biopolymer of marine origin, was used as a stabilizer for fabricating bosutinib nanocrystals. A preliminary screening was done for stirring speed, organic solvent, stabilizer concentration, solvent type, probe sonication time, and probe sonication amplitude (Table 3.2). All studies were conducted at low temperatures (ice-cold water) to decrease drug solubility, promote supersaturation, induce rapid nucleation, and reduce growth kinetics at the particle boundary layer interface (Jiang et al., 2012). It was stirring speed found to directly impact nanocrystal size (F1-F4). This could be due to the more homogenous dispersion of the organic phase when added to the aqueous phase of the stabilizer by the drop-by-drop method responsible for uniform distribution and crystallization aided by ice-cold water. However, the stirring speed of

2000 rpm resulted in more homogeneously dispersed crystals and thus used for further study. The effect of the solvent system was evaluated using coarse drug-dissolving organic solvents like ethanol, methanol, DCM, and chloroform (F3, F5-F7). The methanol was observed to give smallest sized crystals, followed by ethanol, chloroform, and DCM. Methanol has the highest diffusion rate in water, which induced the nucleation of a large number of crystals with small particle size (Jiang et al., 2012). The organic solvent to aqueous ratio was also checked using 2 ml (F5) and 1 ml (F8) for solubilizing the 10 mg drug. The lower ratio (1:5, F5) resulted in the formation of large-sized nanocrystals, probably due to Ostwald ripening, involving dissolution and recrystallization of smaller crystals to give large-sized crystals (Li et al., 2021). However, the effect was minimized by reducing the organic solvent volume using a higher ratio (1:10, F8), which resulted in stable nanocrystals for over one week. A higher ratio resulted in a small particle size due to enhanced supersaturation and reduced Ostwald ripening (Jiang et al., 2012). The effect of stabilizer concentration on nanocrystal size was studied using 0.5, 1, and 1.5 % w/v of fucoidan (F8-F10). Higher fucoidan concentration resulted in smaller-sized crystals, probably due to a faster nucleation rate and decreased interfacial tension upon stabilizer adsorption to the drug surface (Matteucci et al., 2006). However, the difference was not much between 1 and 1.5 % w/v fucoidan. Also, 1 % w/v fucoidan resulted in more uniformly dispersed nanocrystals. In addition, the effect of probe sonication time (F8, F11-F12) and amplitude (F11, F13-F14) was also checked on nanocrystal size and particle distribution. Probe sonication for 10 min at 50 % amplitude resulted in the most uniform nanocrystals of the smallest size. Less sonication time or amplitude resulted in nanocrystals with larger particle sizes, while very high sonication time or amplitude resulted in non-homogenous or bimodal particle distribution.

Table 3.2 Formulation Optimization of Fucoidan Fabricated Nanocrystals.

Formulation	Stirring speed (rpm)	Organic solvent volume (ml)	Stabilizer conc. (% w/v)	Solvent Type	Probe sonication time (min)	Probe sonication amplitude (%)	*Size (nm)	*PDI	Observation
F1	600	2ml	1	EtOH	5	40	3970.23 ± 28.26	1.393 ± 0.236	Non-uniform large crystals
F2	1200	2ml	1	EtOH	5	40	2243.08 ± 35.02	0.528 ± 0.190	Non-uniform large crystals
F3	2000	2ml	1	EtOH	5	40	1257.87 ± 47.19	0.252 ± 0.036	Macro-crystals
F4	4000	2ml	1	EtOH	5	40	1222.74 ± 64.53	0.451 ± 0.032	Macro-crystals
F5	2000	2ml	1	MeOH	5	40	901.34 ± 55.68	0.458 ± 0.057	Microcrystals, Ostwald ripening, unstable post-3-day
F6	2000	2ml	1	DCM	5	40	2440.39 ± 73.19	0.643 ± 0.029	Large crystals

F7	2000	2ml	1	$CHCL_3$	5	40	1478.91 ± 82.36	0.573 ± 0.013	Microcrystals
F8	2000	1ml	1	EtOH	5	40	697.04 ± 22.41	0.266 ± 0.034	Nanocrystals, stable for one week
F9	2000	1ml	0.5	EtOH	5	40	1013.45 ± 54.17	0.129 ± 0.011	Microcrystals
F10	2000	1ml	1.5	EtOH	5	40	789.82 ± 32.02	0.176 ± 0.044	Microcrystals
F11	2000	1ml	1	EtOH	10	40	502.67 ± 12.97	0.285 ± 0.016	Microcrystals
F12	2000	1ml	1	EtOH	15	40	423.04 ± 52.71	0.472 ± 0.033	Microcrystals
F13	2000	1ml	1	EtOH	10	50	149.12 ± 22.36	0.180 ± 0.025	Uniform nanocrystals
F14	2000	1ml	1	EtOH	10	60	100.79 ± 52.67	0.377 ± 0.043	Nanocrystals

**n=3 and data were shown as mean ± standard deviation.*

Therefore, 2000 rpm of stirring speed, 20 ml of 1 % w/v fucoidan as stabilizer concentration, 1 ml organic solvent, 10 min of probe sonication time, and amplitude of 50 A were considered as optimum parameters for the formulation of monodispersed bosutinib nanocrystals.

3.6.2. Evaluation of Nanocrystals for Particle and Microscopic Characteristics

The nanocrystals fabricated using stabilizer fucoidan were observed to have particle sizes of about 150 nm. The nanocrystals had a high zeta potential of -43.30 ± 2.51 and a lower PDI of 0.18, which suggested a highly stable monodispersed system. Nanocrystals were found to have a drug content of about 54.50 ± 2.16 %, revealing high payload potential of nanocrystals. The nanocrystals were highly robust to dilution and were stable on same day. Insignificant difference was found in size between various dilutions post a week. However, a slight increase in size was observed post a week (size and PDI for the dilution of 10-fold: 189.1 ± 19.5 nm and 0.245, 20-fold: 191.2 ± 15.2 nm and 0.219, 50-fold: 203 ± 12.3 nm and 0.167). Although, the difference was not much and the formulation had no significant effect of dilution on size. Similar results were observed by Deng et al., 2010 for the robustness of paclitaxel nanocrystals toward dilutions (Deng et al., 2010). The lyophilized powder of bosutinib nanocrystals exhibited high stability towards storage condition, showing no significant change in particle size, PDI, zeta potential and drug content (Figure 3.1 A-D). Lyophilized nanocrystals (pre-storage) had residual moisture content of 0.57 ± 0.04 % that was within the permitted limit (< 1 %) indicating successful lyophilization of nanocrystals (Merckx et al., 2020). The moisture content was 0.65 ± 0.03 % after storage, however the change was not significant showing storage stability of samples.

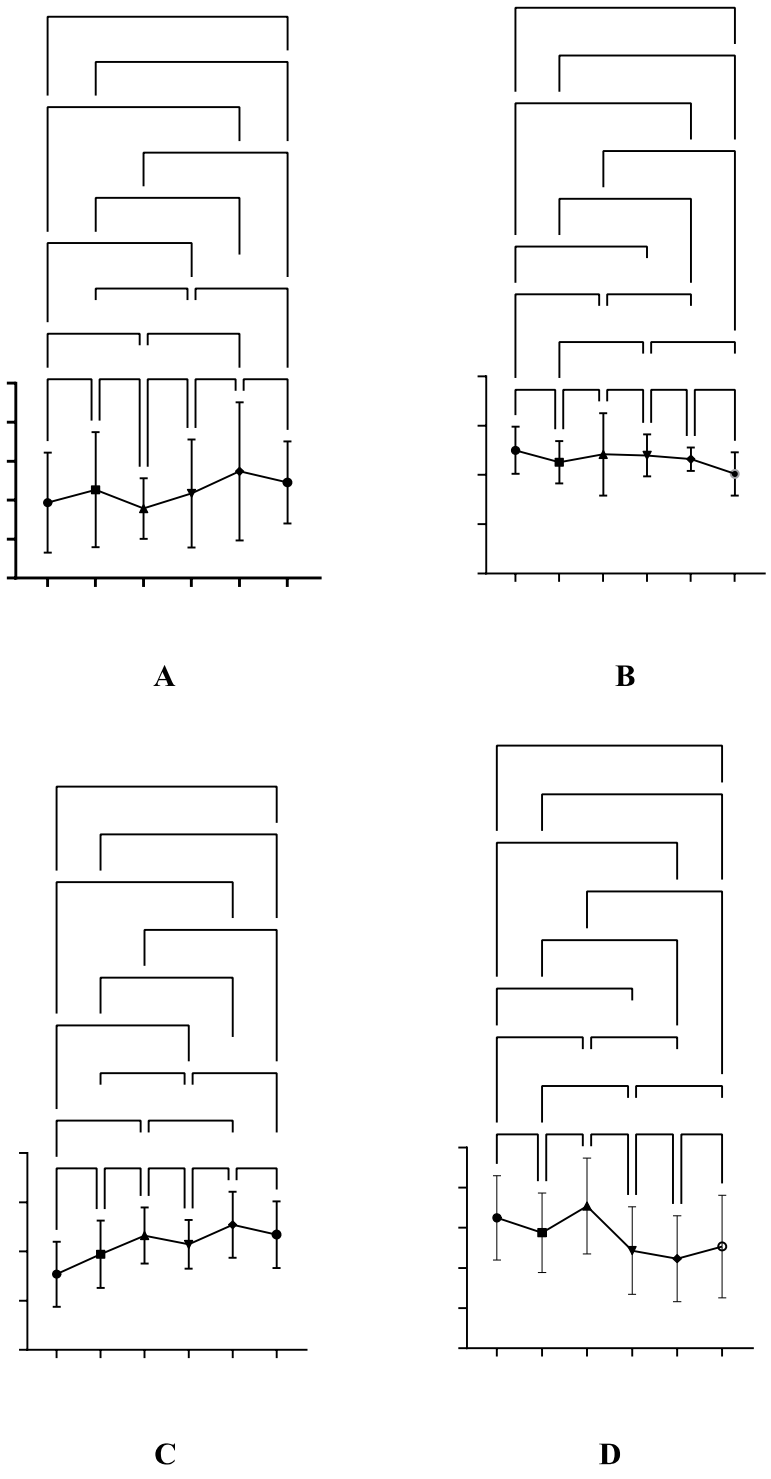

Figure 3.1 Storage stability Graphs for particle size (A), PDI (B), zeta potential (C) and drug content (D). Data were presented as mean ± standard deviation (n=3).

The statistical analysis was done by One-Way ANOVA at significance of p< 0.05. The "ns" denoted non-significant difference.

The nanocrystals were then examined by various microscopic techniques for their shape, size and surface characteristics. The SEM images uncovered the cube-shaped nanocrystals of about 150 nm (Figure 3.2 A). The particles were uniformly dispersed, and the observation was similar to the results observed with DLS. Soisuwan also observed the morphology of cubic anisotropy for clarithromycin nanocrystals (Soisuwan et al., 2019). AFM revealed nanocrystals of similar morphology with a smooth surface (Figure 3.2 B). TEM results also showed cubic-shaped crystals of about 150 nm (Figure 3.2 C). The SED patterns obtained for nanocrystals revealed uniformly dispersed single-phase amorphous rings. The results were in agreement with AFM and XRD results. Similar cube-shaped nanocrystals were also observed in TEM by Wu et al., 2022 for Pluronic F127 stabilized paclitaxel nanocrystals (Wu et al., 2022).

Figure 3.2 Microscopic Investigation of nanocrystals; A) SEM image; B) AFM image, and C) TEM image with Electron Diffraction (SED) Pattern.

3.6.3. Solid State Characterization

The characteristic IR Peak corresponding to nitrile stretching for bosutinib was observed at 2210 cm^{-1} (Levinson and Boxer, 2012). Other characteristics peaks observed were for NH stretching at 3529, 3532, 3465, 3342 & 3235 cm^{-1}; Aromatic CH

Stretching at 3092 & 3008 cm^{-1}; Alkyl C-H stretching 2945 & 2827 cm^{-1}; Weak overtone of Aromatic CH Bend between 2000-1650 cm^{-1}; C-C stretching (in ring) at 1505 cm^{-1}; NH bending at 1597 cm^{-1}; Methylene group CH bending at 1465 cm^{-1}; Methyl group CH bending at 1426 cm^{-1}; Aromatic amine C-N stretching at 1370 cm^{-1}; Alkyl aryl ether C-O stretching at 1247 & 1220 cm^{-1}; C-N stretching at 1050 cm^{-1}; C-Cl stretching at 813 cm^{-1} and NH wag at 726 cm^{-1}. Fucoidan showed characteristic peaks corresponding to broad O-H stretching at 3500-3200 cm^{-1} (3465 cm^{-1}) of monomeric monosaccharides, alkane C-H stretching at 2935 cm^{-1}, C=O stretching at 1765-1565 cm^{-1} (1635 cm^{-1}); S=O stretching at 1330-1190 cm^{-1} (1255 cm^{-1}), alcohol OH bending at 1430-1330 cm^{-1}; S=O stretching at 1165 cm^{-1}, ether C-O stretching 1132 cm^{-1}; ester C-O stretching at 1055 cm^{-1}; and C-O-S stretching at 842 cm^{-1}. The intensity of characteristic peaks for the coarse drug, bosutinib (especially 2210 cm^{-1}) decreased in the physical mixture (pure drug and fucoidan) and nanocrystals (Figure 3.3 A). The probable reason could be due to molecular dispersion of crystalline drug in hydrophilic fucoidan core to give stabilized nanocrystals (Kumar et al., 2019d).

X-Ray Powder Diffraction studies were conducted to determine the stabilizer's effect on the drug's crystalline state after formulation as nanocrystals (Figure 3.3 B). Coarse drug (BTB) exhibited characteristics peak at 2θ = 8.519º, 9.131º, 18.337º, 21.131º, 22.221º, 23.018º, 25.459º, 26.947º, 27.226º, and 29.524º. The stabilizer was observed to have no characteristic peaks and showed a broader diffraction pattern, probably due to the amorphous nature of fucoidan. In addition, the peaks for the drug-stabilizer physical mixture were observed at 2θ = 8.568º, 9.175º, 14.318º, 18.454º, 19.109º, 19.432º, 20.428º, 21.204º, 22.323º, 23.033º, 23.953º, 24.952º, 25.225º, 25.817º and 29.535º. The intensity of peaks, especially at 2θ = 8.568º, was reduced compared to the drug peak at 2θ = 8.519º. Also, a slight shifting in 2θ towards the right was observed. The decrease

in intensity and shifting in peak position can be due to non-homogeneous drug distribution in the stabilizer matrix. In addition, the peaks observed at positions other than 2θ for pure drugs were of stabilizer and very low intensity. The peaks observed for FBNC were also of very low intensity and slightly right-shifted to 2θ = 8.612º, 18.576º, 21.758º, 22.227º, 22.466º, 22.597º, 22.963º, 23.160º, 25.756º, 27.101º, 27.544º, and 29.357º. The probable reason was formation of fucoidan stabilized nanocrystals with a new material structure. The shifting in peak can be due to a decrease in particle size while reduction in intensity was attributed to conversion of crystalline coarse drug to amorphous structure. The DSC curve for BTB showed a sharp endothermic peak at 85 °C. The polymer fucoidan had an exothermic peak at 259 °C. At the same time, the physical mixture and FBNC had no such endothermic peak but an exothermic peak of polymer (Figure 3.3 C). This can be due to the stabilizer fucoidan-driven amorphous phase surrounding the drug's crystalline phase (Silva et al., 2023). Additionally, absence of weak transition or endothermic peak near 0 °C suggested the absence of water traces in prepared nanocrystals. Thus, XRD and DSC studies confirmed the conversion of crystalline drugs into amorphous particles as nanocrystals.

The fabrication of fucoidan stabilized bosutinib nanocrystals was further confirmed by a detailed elemental analysis for S2p, C1s, N1s, O1s, and Cl peaks in XPS spectrum (Figure 3.3 D). The atomic percentages of C1s, O1s, N1s, and Cl2p in BTB were 76.45 %, 21.18 %, 2.26 % and 1.76 %, respectively. For FBNC, the atomic percentages of C1s, O1s, N1s and S2p were observed as 60.54 %, 29.69 %, 8.16 % and 1.62 %, respectively. Masking of Cl2p was due to molecular dispersion of BTB in fucoidan core while S2p percentage was due to fucoidan on nanocrystals surface. The XPS spectra of fucoidan was similar to FBNC due to same elemental composition. A slight alteration in peak intensity (atomic percentage of C1s, O1s, N1s and S2p were 59.48 %, 30.78 %,

6.38 % and 1.82 %, respectively) was observed attributed to physical interaction of bosutinib with fucoidan, however the difference was not significant. This confirmed the successful fabrication of bosutinib nanocrystals with fucoidan.

Figure 3.3 Solid-state characterization of coarse drug (BTB), fucoidan (FP), physical mixture of BTB:FP (FBPM), and nanocrystals (FBNC); A) Infrared spectrum, B) XRD diffractogram, C) DSC thermograms, and D) XPS spectrum.

The ^{13}C CPTOSS solid-state NMR spectra of coarse drug, fucoidan and nanocrystals was determined, as shown in Figure 3.4. Fucoidan revealed a characteristic peak for C

of the –CH3 group in an upfield region of 13.62 ppm (α-l-fucose-C6) and an anomeric carbon peak for C in a downfield region of 95 ppm (α-l-fucose-C1). The O-acetyl group's acetylated moieties (C=O) appeared downfield at 170 ppm. In comparison, pyranoid ring carbons C2-C5 appeared in a region of 58-77 ppm, depicting a complex structural pattern of monomer configuration, glycosylation, and sulfated patterns. The observations were close to 13C NMR spectra reported for fucoidan from *T. conoides* (Alwarsamy et al., 2016). The peaks showed several degrees of multiplicity owing to various glycosidic linkages and sulfation patterns, typically for an α-fucopyranoside backbone. The ^{13}C CPTOSS Solid-state NMR of the coarse drug revealed characteristics peaks at 25.4 (C26), 42.05 (C34), 48.89 (C21, C29, C33), 51.28 (C23), 52.66 (C30, C32), 54.53 (C27), 65.23 (C25), 81.71 (C9), 100.3 (C6, C13), 106.95 (C3), 109.97 (C15), 111.94 (C5, C35), 119.69 (C17), 128 (C16), 132.95 (C12), 143 (C4), 145.56 (C8), 147.21 (C1), 150.92 (C14), 151.99 (C10), and 152.30 (C2). While ^{13}C peaks for FBNC were observed at 24, 42.39, 42.88, 52.41, 64.42, 66.09, 98.87, multiple small peaks between 105-120, 126.87, 127.37, 143.08, 143.64, 147.40, and 151.30. The spectra of FBNC differ from coarse drug spectra in peak number, position, width, and relative intensities. As a general trend, signals in FBNC were broader compared to narrower peaks with coarse drug, attributed to the stabilizer used to formulate FBNC. Results of solid-state NMR suggested the formation of an amorphous material with different degrees of order, probably due to the coating of coarse drug crystals with fucoidan. Similar results were observed in solid-state NMR for curcumin-loaded hydrophilic polymer-based micelles (Pöppler et al., 2019).

Figure 3.4 The ^{13}C CPTOSS solid-state NMR spectrum of A) coarse drug (BTB), B) fucoidan (FP) and C) nanocrystals (FBNC).

3.6.4. Water Contact Angle

The coarse drugs bosutinib belongs to BCS Class IV and is hydrophobic in nature. The hydrophobic drugs on pulmonary administration are generally cleared from the lungs by ciliary clearance or macrophage uptake. Therefore, hydrophobic drugs must be converted to a highly soluble form using a hydrophilic polymer to increase their wettability. Herein, the hydrophobic coarse drug and hydrophilic polymer fabricated nanocrystals were evaluated for their affinity toward water using a drop of SLF. The results revealed a lower contact angle of about 23˚ for nanocrystals compared to the coarse drug showing a higher contact angle of 83˚ with water (Figure 3.5). Lower contact angle attributed to hydrophilic fucoidan used for nanocrystal fabrication that improved wettability of drug. Jiang et al., 2012 also observed a lower contact angle of 23˚ for F68 stabilized simvastatin nanocrystals to improve the wettability of coarse simvastatin (Jiang et al., 2012). The study thus confirmed the conversion of the hydrophobic drug to an amorphous state, which can significantly enhance the solubility or dissolution of the drug in lung fluid to avoid their clearance and increase bioavailability.

Figure 3.5 The water contact angle of A) Coarse drug (BTB) and B) hydrophilic fucoidan-stabilized nanocrystals (FBNC).

3.6.5. BET and Saturation Solubility

The BET study was conducted to determine the effective surface area of the drug responsible for the aqueous and saturation solubility of the drug. The pure drug exhibited a surface area of about 2.5 $m^2 g^{-1,}$ while nanocrystals were found to have a surface area of about 30 $m^2 g^{-1}$, as measured by BET analysis (Figure 3.6 A & C). Nanocrystals significantly increase the surface area due to their nano size. As a result, gas adsorption was significantly improved to about 300 $cm^3 g^{-1}$ compared to the coarse drug with a low nitrogen adsorption capacity of only 25 $cm^3 g^{-1}$ (Figure 3.6 B & D). The saturation solubility of nanocrystals was also studied in SLF to determine the effect of nanocrystals' size-dependent surface area on drug solubility. The nanocrystals were found to significantly increase the saturation solubility of the drug (122.1327 ± 12.563 μg/ml) by ten folds compared to the coarse drug (13.240 ± 4.914 μg/ml) (Figure 3.6 E). The Ostwald-Freundlich equation can explain increased solubility, as it suggests that the particle size reduction results in an increased surface area exposed to media responsible for larger dissolution pressure and, thus, saturation solubility (Sharma et al., 2016). This suggested the role of drug nanocrystals in increasing the effective surface area of the hydrophobic drugs responsible for enhancing the aqueous solubility of drugs and, thus, drug absorption.

3.6.6. In-Vitro Drug Release in Simulated Lung Fluid

The drug release study was carried out in SLF (Figure 3.6 F) to determine effect of fabrication of hydrophobic BTB as nanocrystals for improving the drug dissolution. The coarse drug showed a low drug dissolution rate as compared to nanocrystals. The cumulative percentage dissolution was only 6.5 % for the coarse drug within six hours. The dissolution significantly increased to about 60 % for nanocrystals within six hours. The nanocrystals showed about 70 % cumulative drug dissolution within 12 h.

Compared to nanocrystals, the coarse drug showed only 10 % of cumulative drug dissolution in same time, attributed to its hydrophobicity. The nanocrystals showed almost complete drug dissolution in 48 h due to the hydrophilic property rendered by fucoidan. At the same time, the coarse drug (BCS Class IV) showed only about 12 % drug dissolution due to limited solubility in SLF. The enhanced drug dissolution by nanocrystals was due to the hydrophilic stabilizer used for nanocrystals fabrication, particle size in nano-range and enhanced total effective surface area (He et al., 2020b). The study suggested that nanocrystals can efficiently improve the drug dissolution in lung fluid on pulmonary administration, thereby improving drug bioavailability.

Figure 3.6 A-D) BET Isotherms for surface area analysis of nanocrystals (FBNC) compared to coarse drug (BTB); E) Saturation solubility; F) In-vitro drug release profile in SLF, and G) In-vitro diffusion study across simulated mucus of coarse

drug (BTB) and its nanocrystals (FBNC). Data were presented as mean ± standard deviation (n=3) and statistical significance was denoted as "**" for $p < 0.0001$, and "***" for $0.001 < p > 0.0001$.**

3.6.7. In-Vitro Mucus Diffusion

An in-vitro mucus diffusion study was conducted to determine the capability of nanocrystals to diffuse the respiratory mucus layer compared to coarse drugs. A very low concentration of coarse drug (4.010 ± 0.560 µg/ml) diffused across the simulated mucus membrane within one hour (Figure 3.6 G). However, conversion of crystalline coarse drug to nanocrystals significantly increased the drug diffusion (29.517 ± 0.808 µg/ml in 1 h) across the membrane. The nanocrystals assisted the drug diffusion attributed to their nanosize. Within six hours, the drug concentration reached 59.182 ± 1.035 µg/ml for nanocrystals than coarse drug (10.156 ± 0.655 µg/ml). The nanocrystals significantly enhanced the diffusion by six-folds. Additionally, the nanocrystals were observed to permeate the simulated mucus in its intact form, as observed by DLS. Therefore, nanocrystals, owing to their size, can efficiently diffuse the mucus layer in their intact form or dissolve in the lung fluid lining of internal lung surfaces to release the free drug, readily available for uptake by cancer cells. Similar results were observed for curcumin nanocrystals of about 200 nm that improved the mucus penetration of the drug (He et al., 2020b). The nanocrystals thus can minimize ciliary clearance or macrophage uptake and thus increase uptake by cancer cells (Park et al., 2017).

3.6.8. Powder Flow Property

Dry powder for inhalation (DPIs) should have an appropriate flow to facilitate powder transfer during filling and processing in capsules, as well as transfer from the inhaler device to the lung. Bosutinib nanocrystals (FBNC) had a cone angle of repose of 29.73

± 1.85˚, indicating good flowability. Thus, prepared nanocrystals as dry powder had an adequate flowability that would ease processing and demonstrated their appropriateness for administration as DPIs.

3.6.9. In-Vitro Aerosolization Performance

The aerosolization of FBNC compared to BTB was first determined using twin-stage impinger, apparatus A (TSI), *i.e.,* an artificial lung model. The emitted dose is dependent upon the flow property of formulations. Herein, nanocrystals exhibited an emitted dose (ED) of 67.23 ± 2.5 %, showing the fraction successfully deliverable to the upper and lower lungs. The ED value was attributed to uniformly dispersed FBNC with high stability towards aerosolization and good flow property. The undelivered fraction was due to the high contact angle-dependent adhesion of nanocrystals to the sides of the delivery assembly (device, capsule, mouth, and trachea) (Drumond et al., 2014). The fine particle fraction (FPD) was 40.66 ± 2.51 %, showing nanocrystals' potency in delivering drugs to the lower lungs. The respirable fraction (RF) for nanocrystals was about 60.58 ± 5.39 %, sufficient to deliver the inhaled particles to the lungs. It thus demonstrated the good capability of nanocrystals in delivering drugs to the respirable region of the lungs.

The aerosolization of nanocrystals was also investigation using eight-stage Anderson cascade impactor (ACI), as shown in Figure 3.7. FBNC exhibited higher distribution to lower stages of ACI indicating suitability of nanocrystals for lung deposition as compared to coarse drug BTB. This could be due to lower particle size and higher flowability of dry powder of nanocrystals. The ED was greater than 90 % suggesting excellent aerodynamic behavior. The FPF value was significantly higher for FBNC (54.23 %) as compared to coarse drug (27.60 %). The FPF value over 50 % is favorable

for pulmonary deposition to lung and thus nanocrystals were suitable for drug distribution to deep lungs (Chvatal et al., 2017).

Figure 3.7 Investigation of aerodynamic performance of BTB and FBNCs powder using Eight-stage Anderson cascade impactor (ACI, Westech Instruments, UK); Bar diagram showing percentage particle distribution at each stage for FBNCs as compared to BTB. Bar diagram was shown as mean ± standard deviation (n=3).

3.7. Conclusion

Biopolymer based nanomedicine for pulmonary delivery is safe and effective in lung cancer therapy. The current work proposed formulation of drug nanocrystals dry powder for pulmonary delivery. Herein, polysaccharide fucoidan of marine origin was exploited as hydrophilic biopolymer for the fabrication of bosutinib nanocrystals (FBNC). Microscopic characterization uncovered the cubic-shaped nanocrystals of about 150 nm with high homogeneity (polydispersity index < 0.3) and smooth surface. The lyophilized nanocrystals were robust to dilution, stable for 6 months at 4 °C and contained approximately 50 % drug. The solid-state characterization of FBNC

including FTIR, XRD, DSC, XPS, solid-state NMR and BET revealed the conversion of crystalline bosutinib to nanocrystals with about 10-fold increase in surface area and saturation solubility. An in-vitro drug release study in simulated lung fluid showed over five-fold improvement by nanocrystals than coarse drugs. The mucus permeation efficiency of nanocrystal also increased over five-times than coarse drug. The flow property analysis and aerosolization investigation revealed excellent flowability and good aerosolization performance (ED: 70-80 % and FPD: 40-60 %) indicating the nanocrystals capability in drug delivery to deep lungs. In conclusion, polysaccharide fucoidan stabilized bosutinib nanocrystals can be a novel anticancer formulation for pulmonary administration as dry powder for inhalation for localized lung cancer therapy.